

Impact Factor 6.1



# Journal of Cyber Security

ISSN:2096-1146

Scopus

DOI

Google Scholar



More Information

[www.journalcybersecurity.com](http://www.journalcybersecurity.com)



Crossref

doi



Google Scholar

scopus

## Advanced Converter-Based Control for Power Quality Improvement in PV–Battery Grid Integration

**Dilip Chauhan<sup>1</sup>, Satyam Kumar Upadhyay<sup>2</sup>, Sarvendra Kumar Singh<sup>3\*</sup>**

<sup>1</sup>Electrical Engineering Department, UNS institute of Engineering and Technology, Veer Bahadur Purvanchal University, Jaunpur, Uttar Pradesh, India-222003.

<sup>1</sup>Electrical Engineering Department, UNS institute of Engineering and Technology, Veer Bahadur Purvanchal University, Jaunpur, Uttar Pradesh, India-222003

<sup>3</sup>Department of ICE, Netaji Subhas University of Technology, Dwarka, New Delhi, 110078, India.  
(Corresponding Author): Sarvendra Kumar Singh

**Abstract:** This paper presents an analytical study on efficient power flow control in grid-connected photovoltaic and battery systems, emphasizing their capability to enhance power quality and ensure stable grid interaction. A comprehensive model is developed in MATLAB/Simulink, integrating PV generation with battery storage and shunt compensation to regulate voltage, mitigate harmonics and maintain optimal power exchange with the grid. The PV array is operated under variable irradiance conditions while the battery compensates for fluctuations through controlled charging and discharging. A robust maximum power point tracking (MPPT) algorithm ensures rapid convergence of the PV operating point enabling effective utilization of solar energy. The battery–converter interface is analyzed for voltage stability and current dynamics during abrupt load changes. Shunt inverters are investigated for reactive power support and harmonic suppression contributing to enhanced voltage regulation at the point of common coupling. Simulation results confirm that the proposed control framework achieves efficient power balancing among the PV array, battery and utility grid even under transient disturbances. Grid voltage and current waveforms remain well-synchronized and load-side power quality is preserved despite nonlinear demand. The study demonstrates that coordinated operation of PV and battery resources, supported by advanced control of interfacing converters provides a resilient and efficient solution for integrating renewable energy into low-voltage distribution networks. The findings offer practical insights for designing smart grid systems capable of sustaining reliable power delivery while maximizing renewable energy penetration.

**Keyword:** Solar PV cell, Battery, Inverter, AC Transmission line, Converter, MPPT, ANN, INC, PSO.

### Introduction

The world's energy environment has changed a lot in the last several years because we need to cut down on greenhouse gas emissions, stop using fossil fuels, and switch to renewable energy sources [1]. Photovoltaic (PV) solar systems are one of the most promising and commonly used renewable energy technologies available today. Their flexibility to grow, convenience of use, and quickly dropping prices have led to a huge rise in installations in homes, businesses, and utilities. Even while solar energy has numerous benefits, it has a major drawback: it depends on things like the weather, the amount of sunshine available, and the seasons [2]. Because of this, the power output of PV systems is naturally inconsistent and doesn't always line up with how much energy is being used now.

The universal power quality conditioner (UPQC) has become an important technology for dealing with power quality (PQ) problems, particularly when adding renewable energy sources and electric vehicles (EVs) to the grid [3]. This is because the world of distributed energy systems is always changing. Many studies have suggested different types of UPQC-based voltage source converters (VSCs) that can work with distributed energy resources (DERs) and battery energy storage systems [4]. The goal of these efforts is to reduce voltage fluctuations, current harmonics, and make sure that everything runs smoothly even when the load changes. One of the most recent improvements is the creation of joint optimization-based control methods to enhance PQ [5]. One interesting method used a normalized least mean square algorithm that might also operate as a zero-attractor. This method made it possible for many PV-based VSCs to work together while coordinating with a central energy storage bank. In this setup, the main PV system powers the grid, while additional systems do secondary tasks like buffering and providing reactive power [6]. The system design allows for both vehicle-to-grid (V2G) and grid-to-vehicle (G2V) operations, even when loads behave in a nonlinear way. A bidirectional converter is used to adjust the DC bus voltage, and it does so via proportional–integral (PI) feedback methods [7]. The control strategy can find the basic part of the load current, which helps the control station keep the power flows balanced. In a different setup, an EV charging station included both a UPQC and a superconducting magnetic energy storage (SMES) unit [8]. The dual converter system did a good job of handling PQ on both the supply and demand sides. SMES is different because it stores electrical energy directly as circulating current in a superconducting magnet [9].

This avoids the energy conversion losses that come with thermal or chemical storage. This gives SMES a high round-trip efficiency, frequently over 90%, which makes it a great choice for applications where energy losses need to be kept to a minimum. Some tactics have used grid frequency-based control systems to govern the flow of electricity between PV sources and the grid, particularly when plug-in electric vehicles (PEVs) are plugged in. These systems usually have two

separate parts[10]. One part finds harmonic content in the line current and changes the setpoints for both PV and PEV converters. The other part controls the flow of active power depending on changes in frequency [11]. Together, they make it easier for renewable energy and electric vehicles to be added to the power grid, even when the demand changes and there are harmonic problems. Other research has investigated harmonics utilizing time-domain optimization methods. When the system is running under inductive-resistive (RL) loads, these methods aim to reduce total harmonic distortion (THD) in both current and voltage waveforms [12]. These methods consider how changes in load affect the harmonic content, which makes the response more flexible to changing circumstances. Particle swarm optimization (PSO) and its modified forms have also been used in hybrid cascaded multilevel inverters (HC-MLIs) to find the best switching angles [13]. This lowers the number of strange harmonics in output voltages, which improves the quality of the waveform and the efficiency of the operation. One big benefit of SMES-based energy storage is that it may provide rapid power adjustment without delay since there is no need to switch energy across domains [14].

This characteristic makes SMES great for situations when a quick reaction is needed, such as correcting voltage sags and stabilizing frequency in high-demand situations. A dual-layer DC design has been used in microgrid-based electric vehicle charging systems to connect numerous EVs in parallel [15]. This makes the system more stable and less likely to have voltage dips. These systems also use time-proportional discharge management approaches to make sure that EV charging doesn't stop during grid problems, which helps local PQ goals even more [16]. There have also been big developments in switching control methods. For example, whale optimization algorithms (WOAs) are a kind of metaheuristic optimization approach that have been utilized to create switching sequences in inverter circuits [17]. These strategies cut down on the amount of semiconductor switches needed, which makes the converter more cost-effective without hurting its performance. Compared to older methods that only looked at frequency-domain analysis with restricted harmonic ranges, modern modulation schemes use staircase waveforms to look at all important harmonics [18]. This makes THD mitigation more effective in both single- and multi-phase applications. A predictive phase dispersion modulation (PPDM) approach has been suggested to deal with problems such as voltage sag, swell, and current distortion [19].

This method anticipates how loads will behave in the future and changes modulation tactics to make up for voltage problems on the source side and current harmonics on the load side. Other research has used parallel computing using graphics processing units (GPUs) to speed up the process of finding the best switching angles in complicated inverter systems, especially those with DC source voltages that are not equal [20]. This not only lowers THD but also allows for more inverter levels, which makes the system more flexible and scalable. We have changed selective harmonic mitigation pulse amplitude modulation (SHM-PAM) methodologies to get rid of triplet harmonics, notably in single-phase systems that use five-level inverters [21]. These setups use both shunt and series APFs that are controlled by dynamic switching pulse logic. By adjusting to variations in load-side current, the system keeps the DC link voltage constant which keeps performance stable even when the source voltage circumstances are not balanced [22]. Also, these methods assist control a wide range of nonlinear loads and temporary disturbances, giving full power conditioning even when supply and demand change. Using fuzzy logic controllers (FLCs) and artificial neural networks (ANNs) for dynamic power management in hybrid systems with solar, wind, storage, and electric vehicles is another new idea. These smart controllers make it possible for electricity to flow in both directions via car aggregators, which helps balance energy between the grid, automobiles, and buildings [23]. The FLCs keep the PQ on the load side by turning on compensating mechanisms when they see problems with voltage or current. At the same time, ANNs improve the intelligence of the system by keeping track of the maximum power point (MPP) of renewable sources and sending energy to the right places. There is also a new way to manage the power angle (PAC) that makes the shunt converter's reactive power load easier to handle [24]. By adding the synchronous reference frame (SRF) approach, this technology makes PV-UPQC systems work better by helping them respond to grid problems including voltage drops, load changes, and changing solar irradiation. Reinforcement learning approaches have made this area even better by combining reactive power compensation with template-based current reference [25].

This makes the system more adaptable while keeping the converter ratings low. Power quality in the utility grid is still a big worry because of the increasing usage of power electronics and the rise of distributed energy resources (DERs). Flickers, voltage dips, harmonic distortion, and supply interruptions are all common PQ problems that may make operations less efficient and damage equipment. When EVs are added to this system, they help control frequency, reactive power, and actual power in three primary ways: vehicle-to-grid (V2G), vehicle-to-building (V2B), and vehicle-to-home (V2H). However, UPQC makes it more complicated to link EVs to grid-connected systems in a deeper way. When you manage more than one V2G interaction at the same time, the DC-link voltage changes and puts more demand on the converter infrastructure. If these changes are not correctly managed, they may shorten the life of the battery since it must charge and discharge several times. This shows how important it is to carefully regulate the flow of energy. After making review of the previous study, the key findings are as follows:

- The battery effectively stabilized terminal voltage and managed abrupt current fluctuations (up to 200 A) which proving its robustness for grid-connected applications.
- The proposed hybrid MPPT PSO-ANN-INC consistently tracked the maximum power point under fast-changing irradiance achieving high energy extraction efficiency.

- Grid voltage and current remained sinusoidal, balanced, and synchronized, even with nonlinear load currents demonstrating effective harmonic mitigation.
- The shunt inverter supplied approx. 9 kVAR reactive power steadily, minimized harmonic distortion and maintained sinusoidal output voltages thereby enhancing system stability.
- During transient disturbances the coordinated PV-battery based UPQC system quickly restored steady-state operation, ensuring uninterrupted high-quality power delivery.

The main key contribution of this research work is:

- A novel PSO-ANN-INC hybrid MPPT method is designed which has strength of global search, predictive learning and fast convergence for superior energy extraction.
- The study developed a unified control framework where PV, battery storage and UPQC (series & shunt compensation) work in coordination to regulate voltage, mitigate harmonics and balance power flow.
- Adaptive controllers were analyzed for shunt and series converters ensuring robustness under nonlinear loads and fluctuating solar conditions.
- A full-scale simulation of PV generation, battery interface, UPQC compensation and grid dynamics under realistic disturbances is presented and validated.
- The work demonstrated that how coordinated converter control can enable smart grid applications, support reactive power needs and ensure compliance with IEEE/IEC power quality standards.

### System Description

Maximum Power Point Tracking (MPPT) algorithms are crucial for maximizing the efficiency and output of solar energy installations. A boost converter is used to regulate voltage and ensure optimal power point, especially when connected to a grid. A three-phase voltage source inverter (VSI) with six insulated-gate bipolar transistors (IGBTs) is used as a switching device to control power flow between the direct current (DC) link and the alternating current (AC) grid. This integration ensures synchronization with the grid and seamless power transfer. A hybrid optimization algorithm combining artificial bee colony (ABC) and whale optimization (WHO) techniques are employed to enhance the system's performance and efficiency. This algorithm dynamically adjusts control parameters, ensuring optimal energy conversion under varying environmental conditions. This advanced algorithm improves power quality and stability, compensating for grid fluctuations and disturbances. The grid-tied PV-battery system also incorporates an uninterruptible power quality conditioner (UPQC) for improved power distribution and storage. This system ensures clean, stable, and high-quality power fed into the grid. The use of MPPT and hybrid optimization algorithms significantly improves the overall performance of the PV system, resulting in better energy management, increased power extraction, and enhanced grid stability. **Fig. 1** elaborates on the design and development of system.

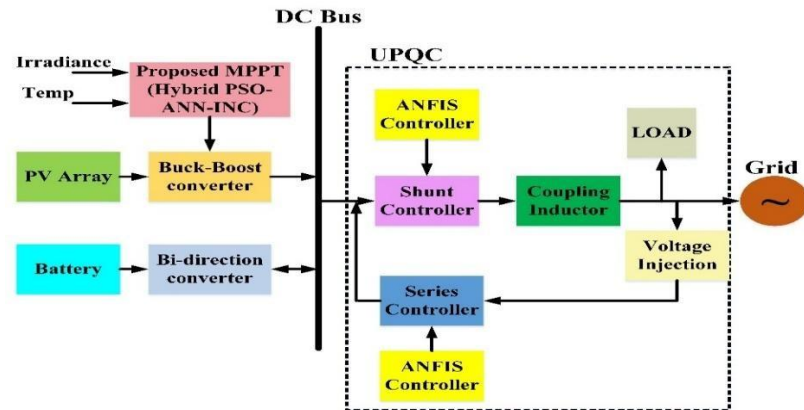


**Fig.1:** Block diagram of system

### Photovoltaic (PV)Module System

The photovoltaic (PV) is highly favorable renewable energy source due to its environmental benefits, abundance and sustainability. It produces electrical energy using solar radiation without emitting the pollutants and greenhouse gases that make it cleaner source of energy. It is sustainable source of energy, but single PV cells do not produce enough electrical energy. So, there are multiple cells that are coupled in series and parallel which form the PV array to produce the electricity. PV array also produces small amount of energy sources [26]. So, the numbers of PV array are connected in series and parallel branches to produce the large amount of electrical energy. In this research article, users define PV array which has 28 parallel strings and 18 series connected modules per string. Each module has 60 cells. Open circuit voltage and short circuit current of each module is 36.3V and 7.84A respectively. This PV array is increasingly integrated with grid system using power improvement devices like unified power quality conditioner (UPQC). A boost converter is employed to match the PV array fluctuating voltage to DC link requirement while a capacitor at DC link acts as an energy buffer to maintaining the voltage stability and supporting dynamic load [27]. An MPPT technique is used for enhancement of the power of PV array. The

current voltage (I-V) relationship of the PV cell can be mathematically expressed using single diode model which is expressed in equation 1.

$$I_{pv} = I_{ph} - I_o (e^{\frac{q(V_{pv}+IR_s)}{nkT}} - 1) - \frac{V_{pv} + IR_s}{R_{sh}} \quad (1)$$

As observed from the equation, the inclusion of series resistance ( $R_s$ ) and shunt resistance ( $R_{sh}$ ) introduce the non-linearities and typically in practical application the value of  $R_s$  is very low and  $R_{sh}$  is large so, their ratio value must be very low value. Hence, their effect may be negligible. By sampling equation 1, the new relationship of V-I will be expressed in equation 2:

$$I_{pv} = I_{ph} - I_o (e^{\frac{q(V+IR_s)}{nkT}} - 1) \quad (2)$$

Where,  $I_{pv}$  is PV current,  $I_{ph}$  is photocurrent (light generated current),  $I_o$  is reverse saturation current,  $q$  is charge on electron,  $V_{pv}$  is output voltage of PV cell,  $n$  is ideality factor of diode whose value is lies between 1 and 2,  $k$  is Boltzmann's constant,  $T$  is absolute temperature in Kelvin.

In **Fig. 2, fig. 2(a)** elaborate the circuit diagram of PV module based on the mathematical equations and **fig. 2(b)** shows the Power-Voltage (PV) and Current-Voltage (I-V) characteristics of PV module.

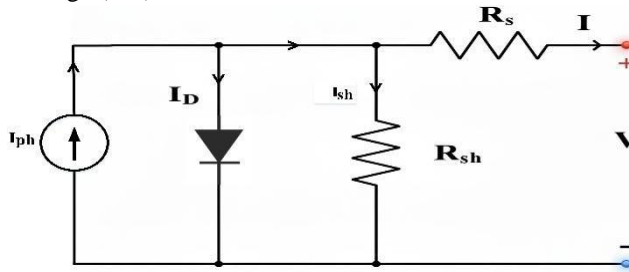


**Fig. 2(a):**PV model based on Mathematical equations

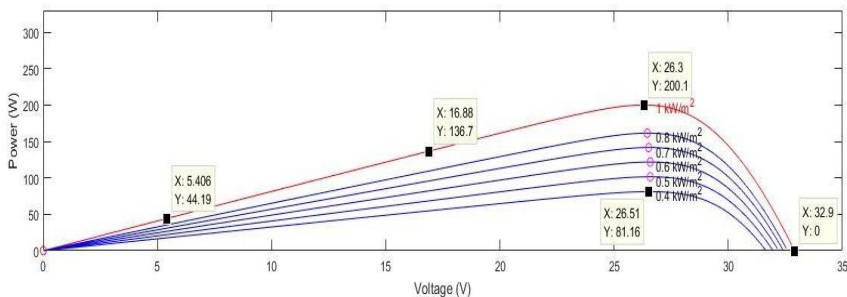
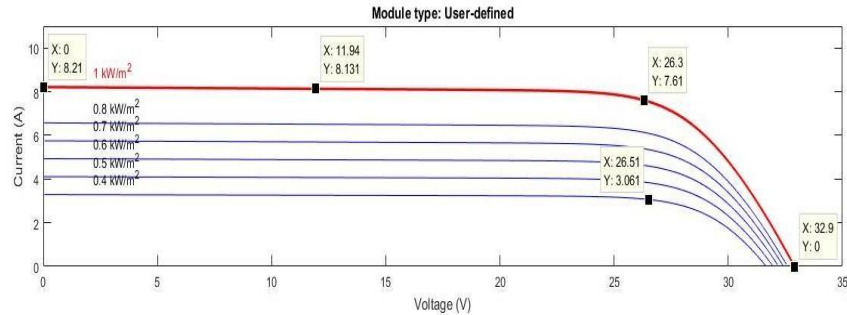


**Fig. 2(b):** Characteristics of PV module

**Fig.2:** Elaboration of PV module

#### Maximum Power Point Tracking (MPPT)

MPPT is more important crucial technique that is used in PV system for ensuring the maximum energy extraction under various environmental and load conditions. Because the output power of a PV system is highly influenced by the different factors such as solar irradiance, temperature, partial shading and electrical properties of connected load. The power generation efficiency of PV module is fluctuating significantly [28]. So, MPPT algorithms are designed to continuously monitor and adjust the operating point of PV array system ensuring that it is operating at maximum power drawing point of PV array where the product of voltage and current drawing from PV system is maximum. There are various MPPT techniques that have been developed and employed on PV system. Each technique has their individual response speeds, complexities, efficiency and these are employed based on specific application requirement. In this research article, the MPPT is used to enhance the efficiency of PV system to maintain the power generation of PV system and monitor the system to

manage the energy [29]. Different techniques have been taken into consideration, from which best one is chosen as shown in **table 2:**

**Table 2:** Different types of MPPT techniques

Technique Name	Advantages	Dis-advantages	Efficiency (%)	Performance
Perturb and Observe (P&O)	Simple, Low cost, easy to implement	Oscillates around MPPT, inefficient under fast changing conditions	95-97	Low
Incremental conductance (INC)	More accurate in dynamic conditions and less oscillation	Requires derivative calculation	96-97	Moderate
Constant Voltage (CV)	No need for complex sensors	Inaccurate during environmental variation and fixed ratio assumption	86-90	Very Low
Short circuit current (SCC)	Cost-effective	Requires disconnection for measurement, interrupts power delivery	85-91	Very Low
Fuzzy logic control (FLC)	Handle non-linearity, uncertain conditions effectively	Requires expert design and tuning	94-96	High
Artificial neural network (ANN)	Learn system behavior, handle based on environment condition	Requires training data and high computation	96-97	Very High
Hill Climbing (HC)	Easy to implement	Instability near Maximum Power Point (MPP)	95-97	High
Particle Swarm Optimization (PSO)	Effective particle shading and finds global MPP	Slower convergence needs tuning and high computation	97-98	Very High
Hybrid INC-PSO	Combines speed and stability and reduces oscillation	Need high switching logic between methods	96-97.5	Very High
Hybrid ANN-INC	Accurate and fast, adapts to changing conditions	Requires high computation time	98-99	Very High
Hybrid PSO-ANN-P&O	Robust in all conditions	Very high complexity and time-consuming tuning	98.5-99	Very High
<b>Proposed MPPT (Hybrid PSO-ANN-INC)</b>	<b>Effective under all environmental conditions, fast and adaptive</b>	<b>Resource intensive, Training requires, Complex logic</b>	<b>99-99.7</b>	<b>Excellent</b>

From the above comparative study, it is found that proposed MPPT which is combination of PSO, ANN and INC algorithm based MPPT is power full and more effective MPPT algorithm under condition. This technique intelligence combines the global optimization capability of PSO, predictive learning strength of ANN and fast local convergence of INC method. The PSO method searches for the near optimal starting point, the ANN quickly adapts to environmental changes by predicting power-voltage relationships and INC ensures precise final tuning of MPP. When these methods are combined together, they create a robust and intelligent system that performs exceptionally well even under rapidly changing irradiance, temperature fluctuations and partial shading conditions. Despite its high computation complexity and need for initial training and its ability to consistently extract maximum energy from PV systems make it more efficient and reliable MPPT solution among modern hybrid approaches. The working flow chart of proposed MPPT is shown in **fig. 3.**

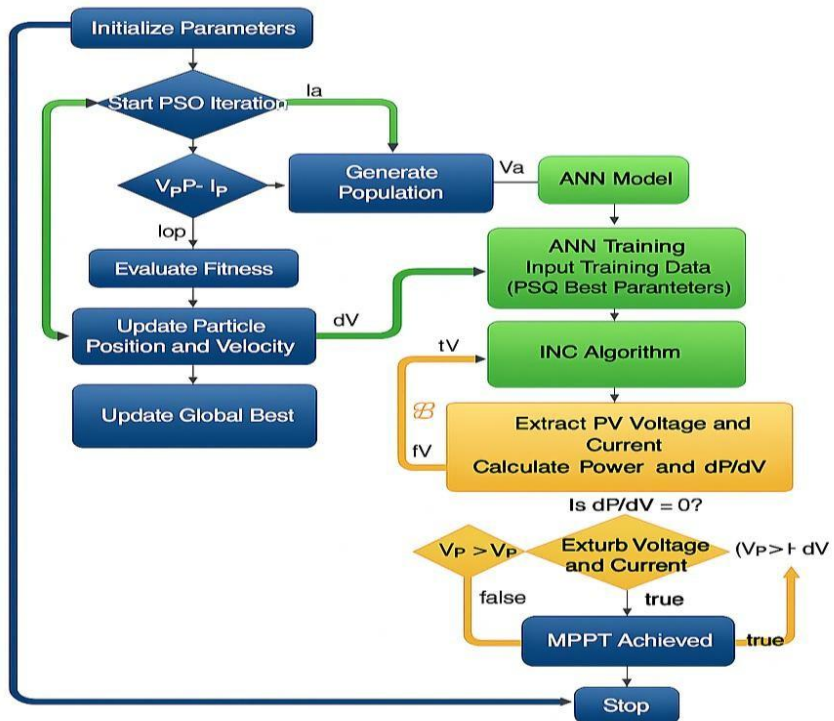


**Fig. 3:** Working flow chart of proposed MPPT

## Battery Pack

A battery pack is a set of battery cells and control circuits that may be put together in different ways to store electrical energy and release it when needed. It is very important for grid-connected photovoltaic (PV) systems, electric vehicle charging stations (EVCS), and unified power quality conditioners (UPQCs) since it helps with energy dependability, storage, and improving power quality. A battery pack is made up of many cells that are connected in series and parallel to reach the appropriate voltage and capacity levels. These cells are generally grouped into modules [30]. A Battery Management System (BMS) takes care of it by keeping an eye on the state of charge (SoC), voltage, current, temperature, and making sure it runs safely by finding faults and balancing the cells. Lithium-ion (Li-ion) and lithium iron phosphate (LiFePO<sub>4</sub>) are two common chemistries because they have a high energy density and cycle life. Superconducting magnetic energy storage (SMES) is another option that works very quickly for important applications [31]. In PV-battery systems, battery packs hold extra solar energy and let it go when there isn't enough sunlight or when demand is high. This helps with energy shifting, increases self-consumption, and makes the grid less important.

## Grid System

The electric power grid is a sophisticated and linked network that makes it possible to generate, transmit, distribute, and use electrical energy. It is the backbone of modern electrical infrastructure, making sure that power from central or distributed generation sources like thermal plants, hydroelectric stations, solar photovoltaics, wind farms, or energy storage systems gets to homes, businesses, and factories safely and reliably. The grid is usually split into three major parts: the production system, which makes energy; the transmission system, which moves high-voltage electricity over vast distances, and the distribution system, which sends lower-voltage power to customers [32]. Smart grids are the next step in the evolution of modern grid systems. They use sophisticated technologies including real-time monitoring, automated control, two-way power flow, demand-side management, and the integration of renewable energy sources (RESs) and electric vehicles (EVs). These smart features improve efficiency, resilience, and environmental sustainability, and they also allow utilities and customers to talk to each other in both directions [33]. To keep the system stable and the power quality high, the grid must keep important characteristics including voltage level, frequency stability, power factor, and harmonic distortion within set limits. Power quality enhancement devices including UPQCs, STATCOMs, and energy storage systems are needed because of problems such load changes, non-linear loads, dispersed generation unreliability, and system failures.

## UPQC to make the Power more Effective

The Unified Power Quality Conditioner (UPQC) is a complex and integrated power electronics-based device that is meant to improve power quality (PQ) in distribution systems. It is especially useful in places where there are non-linear loads, renewable energy sources, and bidirectional energy flow, like photovoltaic (PV) systems, electric vehicle charging stations (EVCS), and smart micro grids. Voltage sags, swells, harmonics, flickers, and unbalanced loads are all examples of power quality issues that may have a big impact on the performance and durability of both utility and consumer-side

equipment. The UPQC solves these problems by putting together the functions of a series active power filter (APF) and a shunt active power filter into one small system with a common DC-link. The series APF is wired in series with the supply and fixes problems with voltage, such as sags, swells, and harmonic distortion. The shunt APF is wired in parallel with the load and fixes problems with current, such as load unbalance, reactive power compensation, and current harmonics [34]. The UPQC operates by adding compensating voltages and currents to the system in real time. This makes sure that the load gets a clean, sinusoidal supply voltage and that the source does not draw any distorted current. A centralized control system keeps an eye on voltage and current levels all the time to make sure the series and shunt converters work together. This control system might employ several algorithms, such as synchronous reference frame theory (SRF), instantaneous reactive power theory (p-q theory), or adaptive methods like artificial intelligence (AI) and reinforcement learning for changing surroundings. The DC-link capacitor or battery energy storage system (BESS) in the centre lets the converters share energy and lets the UPQC work well in both steady-state and transient settings.

### **ANFIS Controller for Shunt and Series Converters**

The Adaptive Neuron-Fuzzy Inference System (ANFIS) controller combines the best parts of fuzzy logic and neural networks to create a very powerful hybrid approach. This makes it perfect for handling the complicated control needs of shunt and series converters in Unified Power Quality Conditioner (UPQC) systems. Traditional controllers rely on exact system models and fixed tuning parameters. ANFIS, on the other hand, can adapt to changing conditions by learning from input-output patterns and updating control rules in real time. This is particularly important when the loads change quickly, there is a lot of harmonic content, and the renewable energy inputs change [35]. ANFIS is very important for controlling the flow of current and keeping the voltage levels steady throughout the load in the shunt converter. The controller changes the output to lower current harmonics and offers reactive power support by constantly checking things like supply current distortion and voltage volatility. The main goal of ANFIS control for the series converter is to fix voltage problems and get rid of harmonic content that comes from grid problems or non-linear loads [36]. This makes the voltage waveform more balanced and cleaner, which improves the power factor and lowers the Total Harmonic Distortion (THD). One of ANFIS's best features is that it can change control settings on the fly by learning and adapting, without needing a detailed mathematical model of the system. Because of this, it works very well in real-world power systems where the circumstances are not always the same or are always changing. In general, ANFIS-controlled UPQCs work better, make systems more reliable, and provide better power quality. This makes them essential for current smart grids and distributed energy systems.

### **Shunt Converter Control**

The shunt converter in a Unified Power Quality Conditioner (UPQC) is very important for keeping the power quality high since it makes up for problems with the electrical distribution system that are caused by current. The main job of this device is to provide a compensatory current at the point of common coupling (PCC) to offset harmonic currents, unbalanced loads, and reactive power needs. The shunt converter makes sure that the current pulled from the grid stays sinusoidal and in phase with the source voltage. This improves the overall power factor and lowers Total Harmonic Distortion (THD) [37]. To control the shunt converter, you usually must make a real-time current reference and use pulse-width modulation (PWM) to monitor and add the right compensating current. There are many ways to control things, such as instantaneous reactive power theory (p-q theory), synchronous reference frame (SRF) theory, and intelligent controllers like Fuzzy Logic and Adaptive Neuro-Fuzzy Inference System (ANFIS). These controllers take in information such as load current, source voltage, and current error signals, and then create gating signals for the voltage source inverter (VSI). Under dynamic situations, such as unexpected changes in load, voltage imbalances, or harmonic surges, the shunt converter quickly adjusts to keep the current waveform pure and balanced [38]. The converter may also help control the DC-link voltage by balancing the power between the UPQC's series and shunt sides. The shunt converter is very important for systems that use renewable energy sources or charge electric vehicles. It helps reduce the impacts of non-linear loads and makes sure that the system works well with the grid. In contemporary smart grid and distributed generation settings, good management of the shunt converter is important for improving system efficiency, keeping voltage and current quality high, and making sure that power is delivered reliably and stably.

### **Series Converter Control**

The series converter in a Unified Power Quality Conditioner (UPQC) takes care of problems with power quality that are caused by voltage in the distribution system. It is linked in series with the source and load using series injection transformers. Its main job is to make up for voltage problems such as sags, swells, flickers, unbalances, and voltage harmonics. The series converter's job is to make a compensating voltage that, when added to the supply line, keeps the voltage at the load end balanced, sinusoidal, and within acceptable limits, no matter what distortions happen upstream. This is done by constantly checking the supply voltage and figuring out the difference between the distorted source voltage and the reference value that is needed. Different control methods are used to do this, such as synchronous reference frame (SRF) control, instantaneous symmetrical components, and adaptive controllers like Fuzzy Logic, Neural Networks, and ANFIS. These controllers respond quickly and accurately even while things are changing, and they are particularly useful for dealing with

settings with non-linear and unbalanced loads. A voltage source inverter (VSI) that works with pulse-width modulation (PWM) is often used to build the series converter [36]. It sends the compensating voltage via coupling transformers without changing the course of the load current. Also, the series converter helps maintain voltage quality at the point of common coupling (PCC) so that distributed energy resources (DERs) may be easily added to the system. It also protects sensitive loads from voltage problems that happen upstream. The series converter may also help with active filtering and reactive power support in more complex setups. For current smart grids and hybrid energy systems to keep the voltage stable, improve the power factor, lower the Total Harmonic Distortion (THD), and maintain the overall quality and stability of power supply, it is important to be able to regulate the series converter well [37].

### Result and Discussion:

The proposed methodology is rigorously evaluated through a detailed MATLAB/Simulink simulation to enhance power quality in a hybrid energy system integrating solar photovoltaic (PV) and battery subsystems. During the simulation, the PV array operated under a constant irradiance of  $1000 \text{ W/m}^2$  while battery modules provided supplementary support to maintain energy balance. To examine the dynamic response and robustness of the control strategy, power quality disturbances were intentionally introduced at predefined time instants. The temporal profiles of the input powers from the solar PV array and battery demonstrating their individual and combined contributions to the overall energy supply. This simulation framework enables a comprehensive assessment of the system's ability to mitigate power quality deviations, maximize renewable energy utilization and maintain grid stability and reliability under diverse operating conditions.

### Analysis of Battery Voltage and Current Characteristics

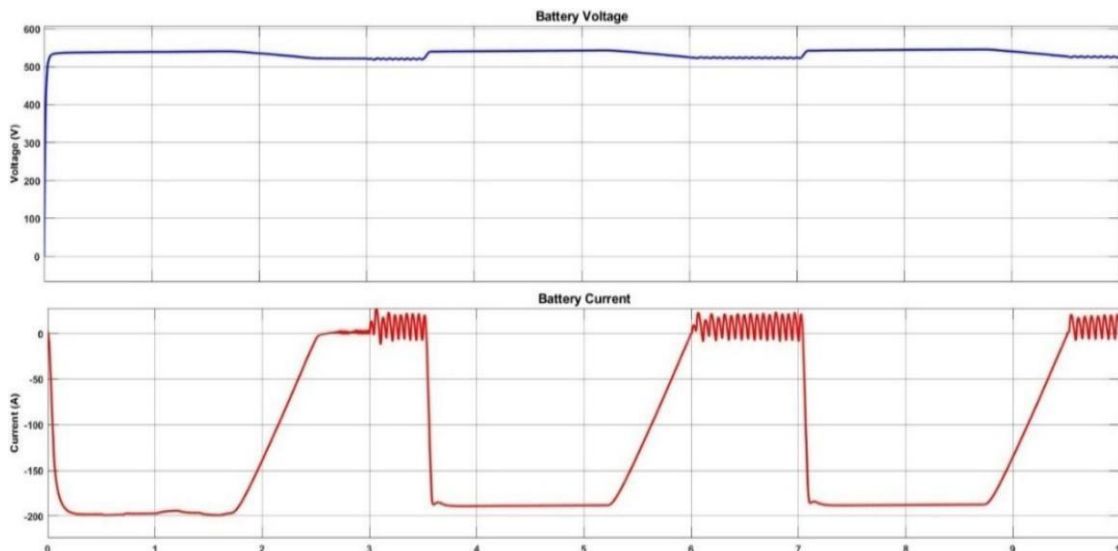


**Fig. 4: Battery Output**

**Fig. 4** illustrates the dynamic behaviour of the battery in terms of voltage and current over a simulation period of 10 seconds. The upper plot represents the voltage profile while the lower plot corresponds to the current response.

The battery voltage exhibits a fast rise at the beginning of the simulation, reaching approximately **520 V** within the first few milliseconds. Thereafter, the voltage remains within the range of **510-550 V**, indicating stable operation under varying current conditions. Minor voltage sags are observed during high discharge periods, followed by immediate recovery once the current transitions to a lower magnitude. These fluctuations are relatively small, highlighting the battery's ability to sustain a stable terminal voltage despite abrupt current variations. This stability indicates that the **state of charge (SOC)** of the battery remains sufficiently high throughout the experiment, allowing it to maintain reliable output characteristics.

The current profile demonstrates a highly dynamic and cyclic nature. Initially, the current drops sharply to around **-200 A**, corresponding to a significant discharge event. Between **2-3 seconds**, the current transitions toward zero and exhibits oscillations, which can be attributed to **transient load switching** or the influence of **power electronic converters**. Similar cyclic patterns are repeated around **3-6 seconds** and **7-9 seconds**, where the current again stabilizes near **-200 A** during discharge and then recovers toward zero with observable **ripple components** during transitions. The oscillations observed in the current waveform are consistent with the switching frequency effects of interfacing converters, reflecting the dynamic interaction between the battery and the external load or charging system.

The combined voltage current behaviour indicates that the battery undergoes multiple load cycles, alternating between periods of heavy discharge (**-200 A** range) and near-zero current with high frequency oscillations. Despite these rapid changes, the voltage remains well-regulated within a narrow band, confirming the **robustness of the battery system and the effectiveness of its power management interface**. The presence of current ripples during transitions suggests **converter induced switching effects**, which are typical in real-world battery energy storage applications.

### Analysis of PV System Performance under Variable Irradiance with MPPT Control

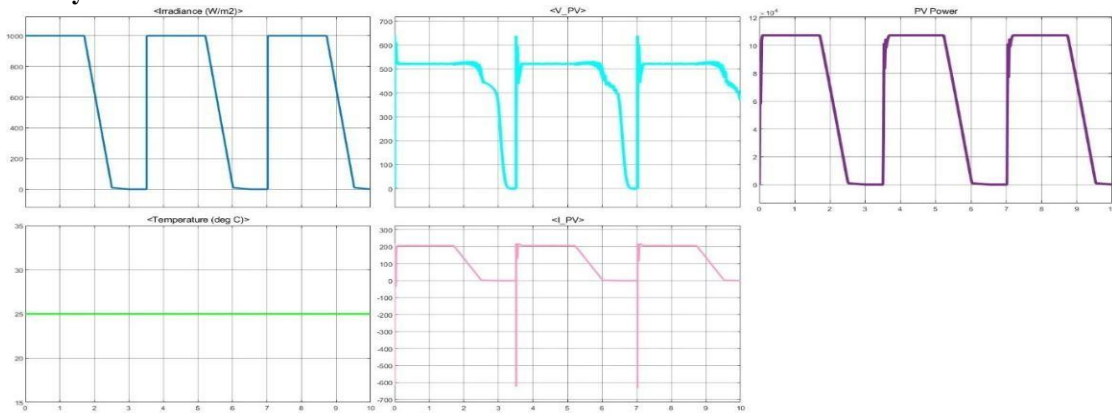


**Fig. 5: Performance evaluation of MPPT**

**Fig. 5** presents the performance characteristics of a photovoltaic (PV) system operating under rapidly changing irradiance levels over a 10 second simulation period. The plots display irradiance, PV voltage, PV current, PV power, and temperature, which together illustrate the dynamic behaviour of the system under maximum power point tracking (MPPT) control.

The irradiance profile (top-left) follows a step-like variation, alternating between **1000 W/m<sup>2</sup>** and nearly **0 W/m<sup>2</sup>**. Such a pattern simulates real-world solar conditions such as intermittent shading and cloud movement. These variations serve as a test scenario for evaluating the effectiveness of the MPPT algorithm.

The PV voltage (top-centre) stabilizes around **500-520 V** during peak irradiance. When irradiance drops, the voltage declines sharply, reaching nearly **0 V** at the lowest points. Voltage overshoots and undershoots occur during transitions, which can be attributed to the control algorithm adjusting the operating point to track the new maximum power point.

The PV current (bottom-right) shows a direct relationship with irradiance. At **1000 W/m<sup>2</sup>**, the current peaks around **200 A**, while it falls close to zero when irradiance is absent. Negative current spikes during transitions are likely linked to switching dynamics of the power converter and rapid adjustments by the MPPT controller.

The PV power curve (top-right) clearly demonstrates the effectiveness of the MPPT algorithm. At maximum irradiance, the system achieves a peak power of approximately  **$1.0 \times 10^4$  W (10 kW)**. When irradiance falls, the power correspondingly decreases to near zero. The sharp recovery of power at each irradiance rise confirms that the MPPT controller quickly relocates the operating point to the new maximum power region.

The PV module temperature (bottom-left) is kept constant at **25 °C**, ensuring that changes in performance are attributed exclusively to irradiance variations. By maintaining fixed temperature conditions, the analysis isolates the impact of solar input on voltage, current, and power outputs.

The observed system response is consistent with the operation of well-established Hybrid MPPT algorithms **PSO-ANN-INC**. Both techniques continuously adjust the operating voltage and current of the PV system to maximize power output under changing environmental conditions. The fast convergence to maximum power following irradiance steps demonstrates the controller effectiveness in handling dynamic scenarios. PSO relies on perturbing the operating point and monitoring power changes, INC directly calculates the slope of the power voltage curve (dP/dV) to identify the MPP. The stable voltage current adjustments in the plots suggest that the chosen MPPT method avoids oscillations around the MPP and responds rapidly to irradiance fluctuations. The results confirm that the PV system, under MPPT control, can efficiently track the maximum power point despite abrupt variations in irradiance. The voltage, current, and power responses align with theoretical expectations, while the constant temperature ensures stable semiconductor properties. This highlights the robustness of the MPPT algorithm in ensuring reliable and efficient energy extraction in real-world solar applications.

### Analysis of Capacitor Voltage Characteristics

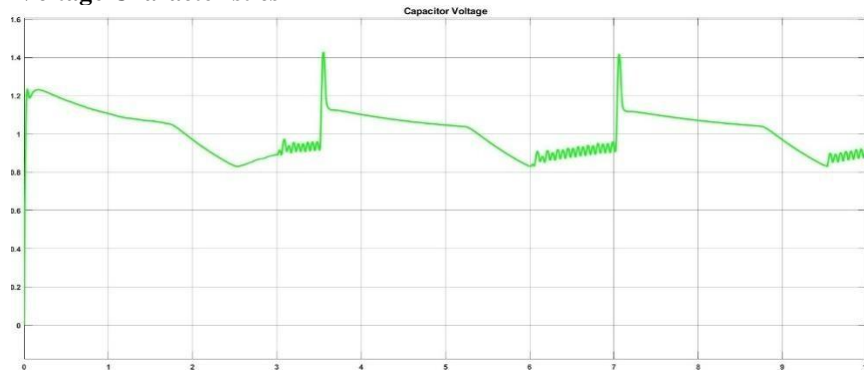


**Fig.6: Capacitor Voltage**

**Fig. 6** shows the variation of capacitor voltage over a simulation period of **0-10 seconds**. The waveform demonstrates the charging, discharging, and transient response of the capacitor under dynamic operating conditions.

At the start of the simulation, the capacitor charges rapidly, and the voltage rises steeply to approximately **1.2 V**. A small overshoot beyond 1.2 V is observed, followed by stabilization. This sharp rise corresponds to the immediate charging of the capacitor when connected to the supply.

After the initial charging, the capacitor voltage gradually decreases from **1.2 V** to around **0.85 V**, representing the discharging phase under load. During this period, small oscillations appear on the waveform, particularly after **2.5 s**, suggesting ripple effects caused by circuit switching or converter operation.

At around **3 s**, a sudden voltage spike occurs, reaching nearly **1.45 V**. This indicates a recharging or switching event within the system. After the spike, the capacitor voltage quickly stabilizes near **1.1-1.2 V** and resumes its gradual discharge trend.

- Between **4-6 s**, the voltage again discharges slowly to about **0.85 V**, with superimposed ripples.
- At **6-7 s**, another sharp spike is recorded, again exceeding **1.4 V**, followed by stabilization near **1.1 V**.
- Beyond **7 s**, the capacitor undergoes a gradual discharge until **9 s**, where the voltage decreases close to **0.9 V**, with ripple disturbances becoming more prominent.

#### Observations

1. **Operating Range:** The capacitor voltage fluctuates between **0.85 V** and **1.45 V** throughout the simulation.
2. **Charging Events:** Sharp upward spikes ( $\sim 1.45$  V) indicate controlled recharging or switching activity at  $\sim 3$  s and  $\sim 7$  s.
3. **Discharge Pattern:** Between spikes, the voltage decreases linearly, showing typical capacitor discharge behaviour under load.
4. **Ripple Effects:** Oscillations superimposed on the waveform suggest the influence of converter switching frequency or dynamic circuit interactions.

The capacitor demonstrates a **cyclic charging and discharging pattern**, with periodic recharging events and ripple disturbances. Despite these transients, the capacitor voltage remains within a stable operating window, highlighting its effectiveness in storing and releasing energy under varying load and switching conditions. This behaviour is characteristic of capacitors used in **power electronic circuits**, where they serve as DC-link or filtering elements to smooth voltage fluctuations.

#### Analysis Shunt Inverter

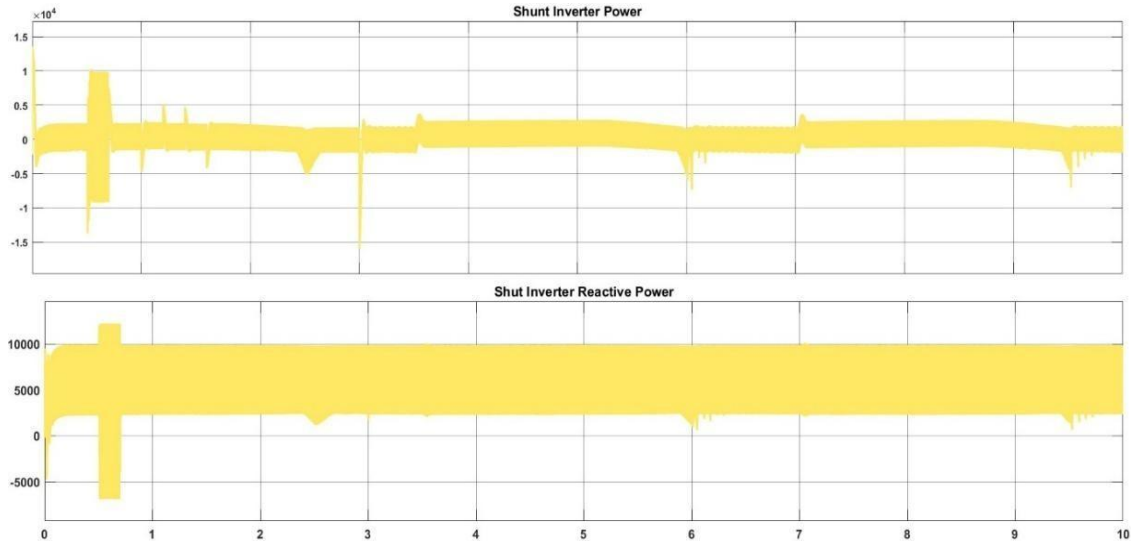


**Fig. 7: Analysis of Shunt inverter power**

**Fig. 7** presents the dynamic performance of the shunt inverter illustrating its active power (upper graph) and reactive power (lower graph) responses over a simulation period of 10 seconds. These plots highlight the inverter's role in power compensation and voltage support under varying system conditions.

The active power response of the inverter shows significant oscillations during the initial transient (0-1 s), reaching both positive and negative peaks around  $\pm 1.5 \times 10^4$  W. This behaviour reflects the inverter's rapid adjustment to initial switching and system disturbances. After the first second, the active power stabilizes close to **zero**, with smaller fluctuations. Occasional sharp spikes, observed near **3 s, 6 s, and 9 s**, correspond to system disturbances or sudden load variations. Overall, the active power trend indicates that the inverter operates primarily as a compensating device, ensuring that the net active power exchange with the system remains minimal.

The reactive power profile demonstrates a more consistent compensating behaviour. During the initial transient (0-1 s), the inverter reactive power fluctuates widely between approximately **-7000 VAR and +11,000 VAR**. Once stabilized, the inverter maintains a nearly constant reactive power output of about **+9000 VAR**, which signifies its continuous contribution

to voltage regulation. However, minor disturbances occur around **2.5 s, 6 s, and 9 s**, where the reactive power briefly deviates before returning to its steady value.

The combined results confirm that the shunt inverter effectively enhances system stability by **absorbing or injecting power as required**. The **active power remains centred near zero** after transients, validating its role in harmonic and disturbance compensation. Meanwhile, the **positive reactive power output** indicates that the inverter supplies reactive power support, thereby contributing to improved voltage regulation and overall power quality. The transient oscillations observed are typical of inverter-based systems and remain within acceptable operational ranges.

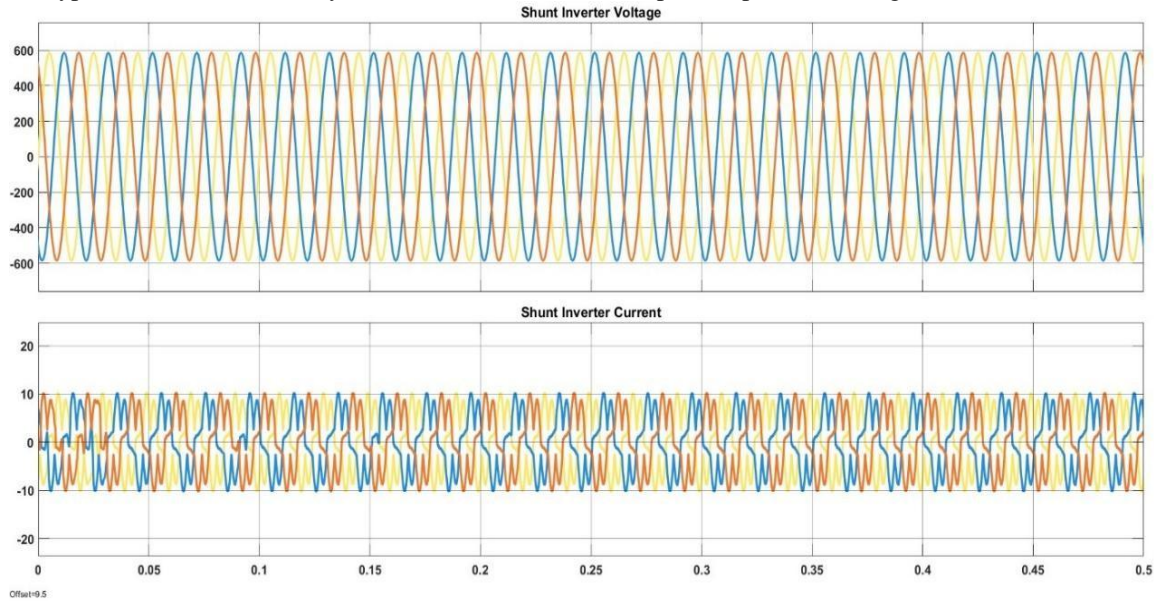


**Fig. 8: Shunt inverter voltage and current**

**Fig. 8** illustrates the dynamic behaviour of a three-phase shunt inverter by showcasing its output voltage and current waveforms under steady-state operation. The plot provides insight into the role of the shunt inverter in maintaining voltage support and reactive power compensation within the system. The upper subplot displays the **three-phase output voltage** of the shunt inverter, representing phases A, B, and C using blue, orange, and yellow lines, respectively. The inverter output voltage is **balanced** and **sinusoidal**, with each phase having a peak amplitude of approximately  $\pm 600$  V. This corresponds to an RMS voltage of around 424 V, which is suitable for interfacing with the grid through a transformer or for direct connection in medium-voltage distribution systems. The waveform maintains a **120-degree phase shift** between each phase, indicative of a well-synchronized and phase-balanced inverter operation. Over the entire observed time span (0 to 0.5 seconds), no distortion, sag, or transients are observed, suggesting the inverter is operating in a stable environment with a properly tuned voltage control loop. This sinusoidal voltage generation is typically achieved using advanced modulation strategies, such as **Sinusoidal Pulse Width Modulation (SPWM)** or **Space Vector PWM (SVPWM)**, ensuring minimal Total Harmonic Distortion (THD) in the output voltage. The lower subplot illustrates the corresponding **output current** of the shunt inverter across the three phases. The current waveforms exhibit **quasi-sinusoidal behaviour**, with evident **harmonic content** and some degree of **ripple**, which is expected due to the **switching nature** of power electronic inverters. The peak current amplitude is approximately  $\pm 20$  A, with varying waveform shapes across the three phases. The distortion and ripple in the current waveform suggest that the inverter is compensating for **nonlinear or unbalanced load conditions**, possibly involving harmonic-rich current demands. Despite the distortions, the current remains balanced in terms of amplitude and phase sequence, indicating that the **control strategy** potentially based on **hysteresis current control** or **predictive current control** is capable of regulating output currents while tracking reference waveforms under dynamic loading conditions.

The shunt inverter, as observed from these waveforms, plays a crucial role in **power quality improvement**. By injecting current into the system in response to voltage sags, unbalances, or reactive power demand, it contributes to **voltage regulation, power factor correction, and harmonic compensation**.

The waveform patterns confirm that the inverter operates with high dynamic performance and stability, capable of generating clean voltage while delivering compensating currents in real-time.

## Analysis of Grid Output Power and Voltage:

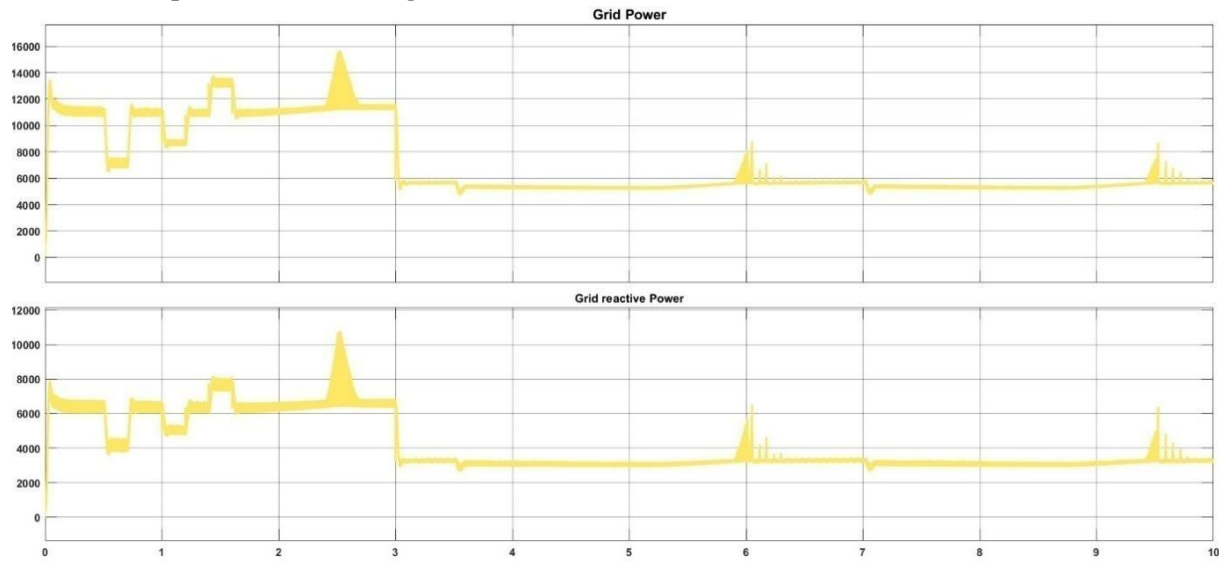


Fig. 9: Grid Power

**Fig. 9** shows the variation of **grid active power** (top) and **grid reactive power** (bottom) over a 10 second interval. These results reflect how the grid responds to changing load conditions and the influence of inverter compensation.

At the start, the grid active power is about **13,000 W**, but it undergoes several fluctuations within the first three seconds. Between **0.5 s and 1.5 s**, the power dips to nearly **7,000 W**, followed by step like rises and drops. A distinct peak of approximately **16,000 W** occurs near **2.7 s**, after which the power decreases and settles around **5,500 W** from **3 s onward**. Beyond this point, the curve remains relatively steady, with small spikes observed around **6 s** and **9 s** before returning to the stable level. The reactive power follows a similar trend. Initially, it is around **7,000 VAR**, but between **0.5 s and 1.5 s**, it falls to nearly **4,000 VAR**, with visible step variations. A sharp rise occurs at **2.7 s**, where the reactive power reaches nearly **11,000 VAR**. After **3 s**, it stabilizes in the range of **3,500–4,000 VAR**, with minor oscillations. Small peaks are again visible at **6 s** and **9 s**, but the system quickly recovers.

The results indicate that the grid experiences significant fluctuations during the early transients but achieves stable operation after **3 s**. The **steady-state active power** (~**5,500 W**) and **reactive power** (~**4,000 VAR**) are lower compared to the initial values, suggesting effective support from the inverter in sharing the load demand. The peaks observed at **2.7 s, 6 s, and 9 s** reflect short disturbances, but the system shows quick recovery, demonstrating reliable power balancing and voltage support from the compensation mechanism.

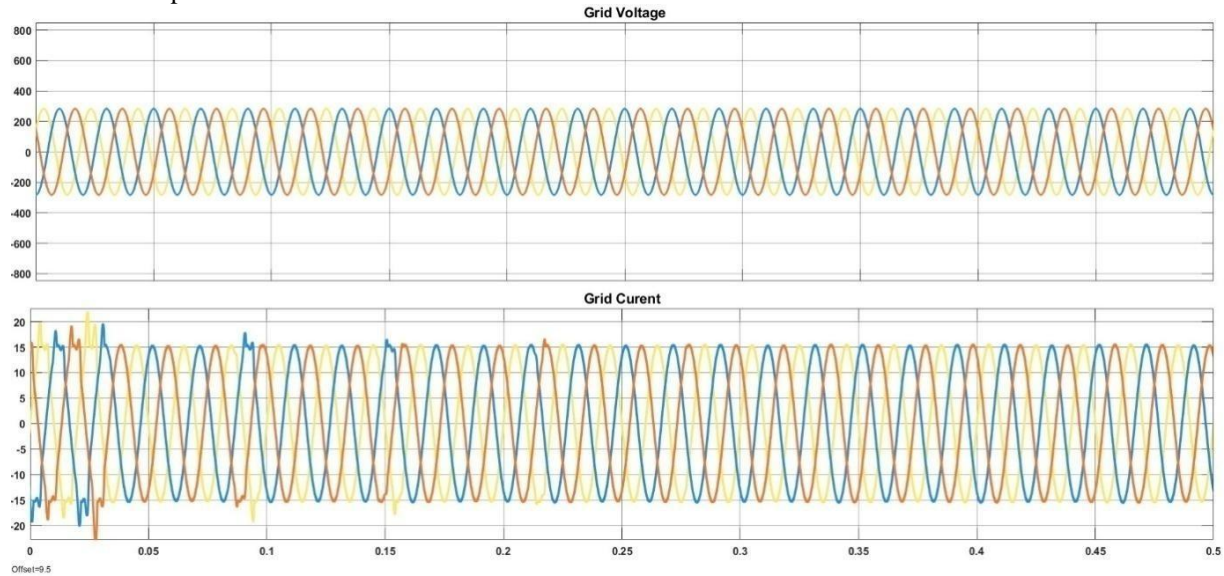


Fig. 10: Grid voltage and current

**Fig. 10** presents the time-domain plots of the three-phase grid voltage and current waveforms recorded over a time duration of 0.5 seconds. The figure is divided into two subplots for clarity: the upper subplot displays the three phase grid voltages, whereas the lower subplot illustrates the corresponding grid currents for each phase.

The grid voltage signals shown in the upper portion of the figure are balanced and purely sinusoidal in nature. Each waveform corresponds to one of the three phases - typically denoted as Phase A (blue), Phase B (orange), and Phase C

(yellow). All three phases exhibit consistent amplitude and frequency characteristics, with a phase displacement of  $120^\circ$  between them, which is indicative of a well-maintained and symmetrical three-phase power supply system.

The peak voltage magnitude for each phase is observed to be approximately  $\pm 325$  V, translating to an RMS (Root Mean Square) value close to 230 V, which is in line with standard low-voltage distribution levels (e.g., 230/400 V systems). Throughout the observed time interval, no visible distortions, unbalances, or voltage sags/swells are present in the waveform. This confirms that the voltage source is of high quality and not influenced by external disturbances or nonlinearities. The clean sinusoidal nature of the voltage waveform further suggests minimal harmonic content and implies the presence of effective grid-side filtering and/or stable utility grid conditions.

The lower subplot illustrates the current waveforms injected into or drawn from the grid for the three corresponding phases. Initially, during the first 0.1 seconds, the current waveforms exhibit noticeable transients and small oscillations. This initial non-sinusoidal behaviour is typical in systems undergoing synchronization, start up, or load connection events. The nature of these transients may be attributed to inrush currents, phase alignment processes, or control loop initialization in grid connected power converters.

Beyond the 0.1-second mark, the current waveforms stabilize into steady-state sinusoidal waveforms. These waveforms closely follow the voltage waveforms in frequency and phase, suggesting proper phase alignment and synchronization between the voltage and current. The current waveforms also remain balanced, with a consistent phase displacement of  $120^\circ$  between each phase, and have an approximate peak amplitude of  $\pm 20$  A. The sinusoidal shape and symmetry of the current waveforms after stabilization indicate the presence of a linear and balanced load, or effective current control in an active power converter.

The waveforms shown in Fig 10 Collectively indicate that the three-phase system operates under **balanced, stable, and controlled conditions**. The voltage source is clean and undistorted, with stable amplitude and frequency, while the current waveforms demonstrate proper dynamic response and steady-state behaviour post-transient.

Such behaviour is particularly important in grid-tied applications, including:

- Renewable energy systems (e.g., photovoltaic or wind inverters)
- Distributed generation units,
- Active power filters or power quality conditioners,
- Electric vehicle (EV) charging infrastructure.

The minimal harmonic distortion and balanced nature of both voltage and current waveforms signify that the system adheres to grid compliance standards such as IEEE 1547 or IEC 61000-3-2/3, ensuring compatibility and non-interference with other grid-connected equipment.

### Voltage Injection for Grid system

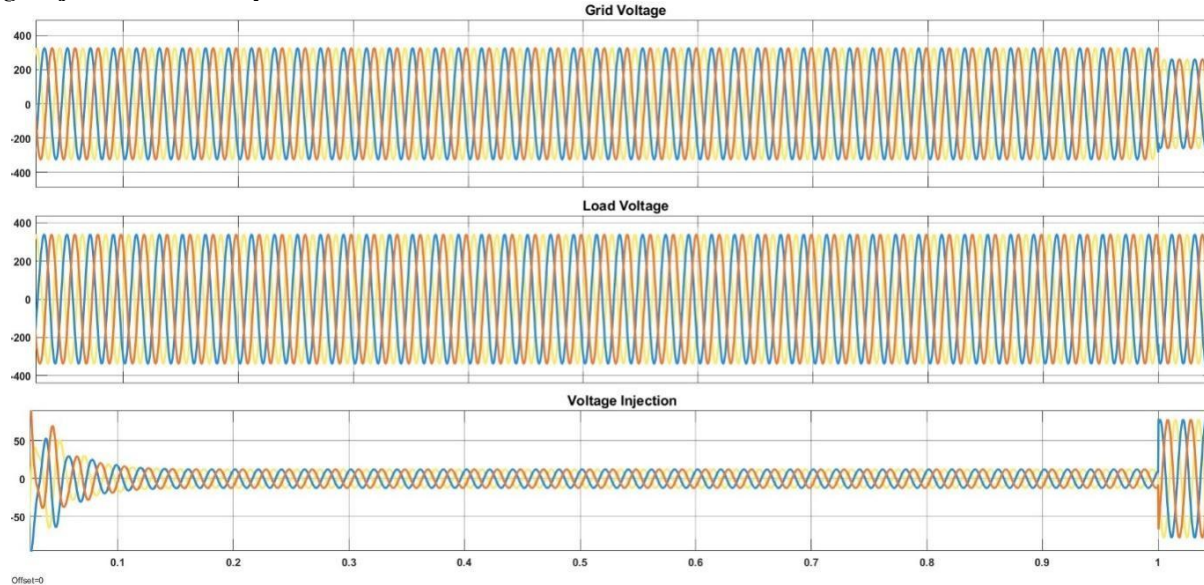


**Fig. 11: Grid Voltage Injection**

**Fig. 10** depicts the dynamic behaviour of the three-phase system voltage at three key locations: the **grid voltage**, the **load voltage**, and the **voltage injected** by the control system. The simulation window spans 1 second, and each subplot represents time-domain waveforms for three phases: Phase A (blue), Phase B (orange), and Phase C (yellow). This figure highlights the effectiveness of voltage injection for disturbance compensation and power quality enhancement.

In the top subplot, the **grid voltage** is shown across three phases. During the majority of the simulation (from 0 to approximately 0.95 s), the grid voltage remains **balanced, purely sinusoidal, and stable**, with a peak amplitude of about  $\pm 325$  V per phase. This corresponds to an RMS voltage of approximately 230 V, which is typical for a standard low-voltage grid.

However, near the end of the simulation window (at  $t \approx 0.95$  s), a noticeable **voltage sag or disturbance** appears. The waveform amplitude decreases suddenly, indicating the presence of a grid-side voltage anomaly. This could be due to a fault, load switching event, or transient disturbance from the upstream source.

The middle subplot presents the **load voltage**, which closely mirrors the grid voltage behaviour for most of the duration. From  $t = 0$  s to  $t \approx 0.95$  s, the load experiences a sinusoidal and balanced voltage similar to the grid, confirming that the system operates in a steady-state condition without external disturbances. However, after  $t \approx 0.95$  s, the voltage disturbance seen at the grid is also reflected at the load terminals, suggesting that the disturbance has propagated downstream and affected the load-side voltage quality.

The bottom subplot shows the **voltage injection** performed by a power conditioning system - most likely a **Dynamic Voltage Restorer (DVR)** or **series compensator** - to mitigate voltage disturbances. The injected voltage is zero or near-zero for the majority of the time ( $t = 0$  to 0.95 s), which is expected during undisturbed operation when no compensation is required.

From the beginning of the simulation, a **transient damped oscillation** is observed, likely corresponding to system initialization. Afterward, the injected voltage remains minimal until  $t \approx 0.95$  s, when a significant voltage injection occurs across all three phases. This response coincides precisely with the onset of the grid voltage disturbance.

The injected waveform has a peak amplitude reaching approximately  $\pm 60$  V, exhibiting a clear sinusoidal shape and balanced phase displacement. The controller dynamically injects the required voltage components to **compensate the sag or imbalance** in the grid supply. This voltage injection ensures that the **load voltage remains close to nominal**, thus protecting sensitive downstream equipment and maintaining power quality.

#### System Behavior and Control Effectiveness

The overall analysis confirms that the control strategy used in the system is both **responsive** and **effective**. The DVR or equivalent compensator accurately detects the disturbance and initiates appropriate voltage injection at the exact moment the sag begins. This injection helps restore the load voltage to its pre-disturbance level, even though the grid experiences a voltage drop.

#### Analysis of Load Response

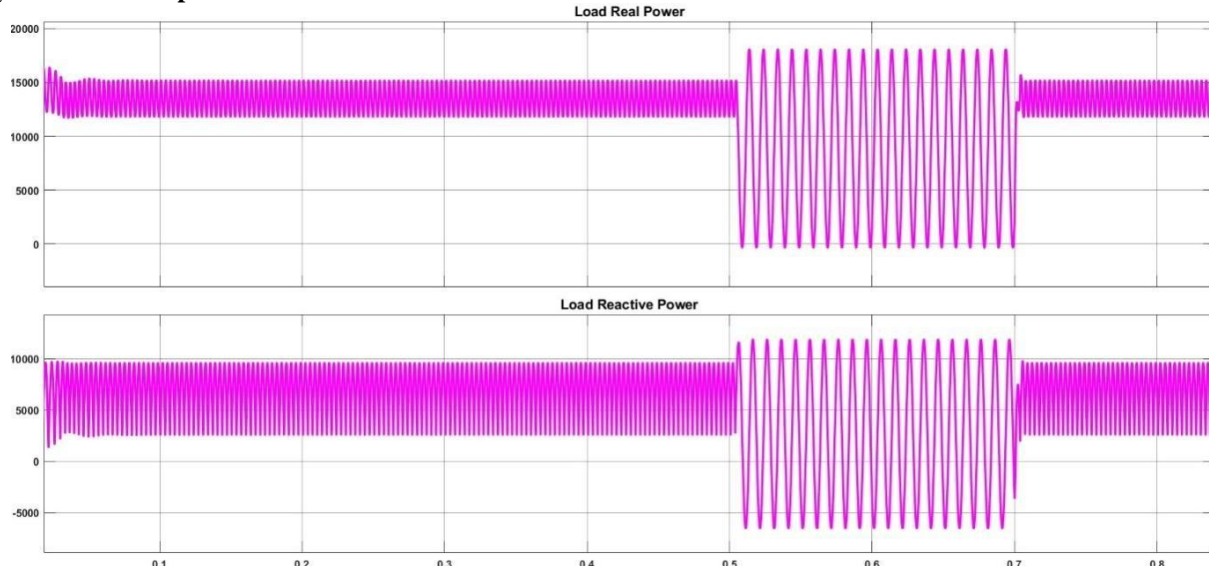


**Fig. 12: Load Power**

**Fig. 12** presents the time-domain response of the load's **real power (P)** and **reactive power (Q)** over a simulation time span of approximately 0.85 seconds. The top subplot illustrates the real power, while the bottom subplot corresponds to the reactive power. Both waveforms are plotted in magenta for visual clarity and comparison.

During the initial phase of the simulation, specifically from  $t = 0$  s to  $t = 0.5$  s, the real power maintains a relatively steady oscillatory profile with an average value centred around **15 kW**. The high-frequency ripple superimposed on the waveform can be attributed to switching operations or internal dynamics of the power electronic interface. This operating point represents the steady-state condition of the system under nominal load.

At  $t = 0.5$  s, the system experiences a significant disturbance, which manifests as a large deviation in the real power waveform. This could correspond to a **step change in load**, **activation of a large dynamic component**, or **mode transition in the power converter**. The real power fluctuates rapidly between approximately **0 W** and **18 kW** during the disturbance period, indicating a highly dynamic and transient operating state. This transition persists until approximately  $t = 0.68$  s. Following this disturbance, the system gradually re-establishes a new steady-state operating condition. From  $t = 0.68$  s onwards, the real power waveform stabilizes with a slightly reduced amplitude of ripple, and the average power remains close to **14.5-15 kW**, suggesting a successful restoration of system equilibrium.

The reactive power response, as shown in the bottom subplot of **Fig 12** follows a similar trend to that of the real power. Prior to the disturbance (i.e.,  $t = 0$  s to  $t = 0.5$  s), the reactive power waveform remains stable with high-frequency switching-induced oscillations around an average value of approximately **7 kVAR**. The waveform is symmetric and indicates a capacitive or inductive nature of the load, depending on the sign convention used.

At  $t = 0.5$  s, a sharp change in the system's reactive power profile is observed, coinciding with the event seen in the real power waveform. The reactive power swings significantly between **+10 kVAR** and **-5 kVAR**, highlighting a substantial change in the load's reactive characteristics. This may result from the connection or disconnection of reactive components such as capacitor banks, filter networks, or inductive devices, or from changes in the power factor control mode of an inverter based resource.

By  $t = 0.68$  s, the reactive power transitions back to a new steady state level with an average value close to **6.5-7 kVAR**, and the oscillations exhibit a more damped response. This implies that the system's reactive power control mechanism successfully mitigated the disturbance and resumed normal operation.

The load power behaviour in **Fig. 12** indicates a system that is dynamically responsive to significant load events or control changes. The observed transient at  $t = 0.5$  s demonstrates the system's ability to handle sudden power variations and recover to a stable operating point within a short period. Such performance is essential in **smart grid environments, renewable energy integration, and converter-based distribution systems**, where load profiles are inherently time-varying and subject to frequent disturbances. The coordinated stabilization of both real and reactive power post-disturbance highlights the effectiveness of the control strategy employed. The rapid damping of oscillations also implies sufficient system inertia, robust converter control, or fast dynamic compensation.

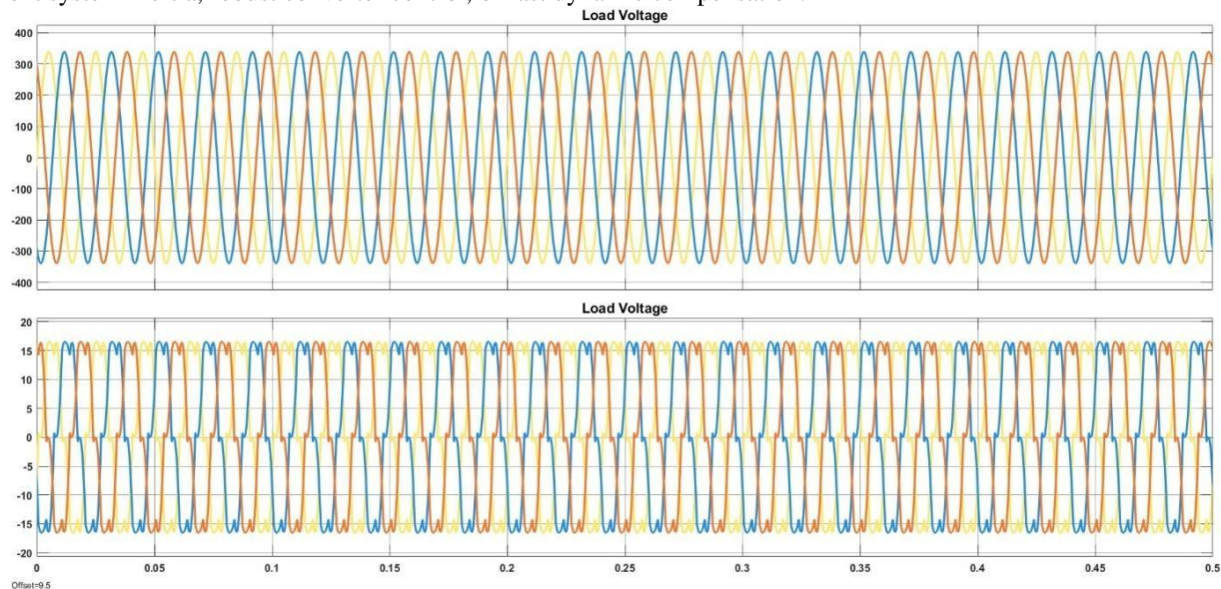


**Fig. 13: Load Voltage and current response**

**Fig. 13** presents the time-domain behaviour of the **three-phase load voltage** and **load current** over a duration of 0.5 seconds. The waveforms are divided into two subplots. The upper subplot illustrates the three-phase voltages applied across the load, while the lower subplot shows the corresponding load currents. Each phase is represented in a distinct colour (commonly red, yellow, and blue for phases A, B, and C, respectively), enabling phase wise observation.

As shown in the top subplot of **Fig. 13**, the three phase load voltage waveforms exhibit a well-balanced and purely sinusoidal nature, with each phase displaced by  $120^\circ$  from the others, characteristic of a healthy three phase system. The voltage amplitude for each phase is approximately  $\pm 325$  V, corresponding to an RMS value of around **230 V**, which is typical for a low-voltage distribution network. The frequency of the waveforms is **50 Hz**, consistent with standard grid operation in many regions. There is no noticeable distortions, overshoots, or phase imbalance throughout the simulation window, indicating that the voltage supply to the load remains stable and undisturbed. This implies that the upstream source or converter system provides high power quality, ensuring reliable voltage delivery to the load.

The bottom subplot displays the three-phase load current waveforms. These current signals are also periodic but differ in waveform shape from the sinusoidal voltages. Unlike the ideal sinusoidal voltage, the current waveforms show **significant distortion**, with sharp peaks and flattening in certain regions. This is characteristic of a **nonlinear load**, such as a power electronic converter, rectifier-fed system, or harmonic-producing device. The peak current for each phase is approximately  $\pm 18$  A, with high-frequency switching components visible, indicating the presence of **fast-switching power converters** or **pulse width modulation (PWM)** techniques used at the load side. Despite the distortion, the three-phase current waveforms remain balanced in magnitude and phase separation, suggesting symmetrical operation. The offset value mentioned (Offset = 9.5) in the image metadata may refer to the numerical or visual adjustment applied during plotting to enhance visibility between signals. It does not affect the actual waveform shape or electrical behaviour.

The comparison between voltage and current waveforms reveals a classic case of **nonlinear current drawn from a sinusoidal voltage source**. While the voltage remains undistorted and sinusoidal, the load currents are significantly non-

sinusoidal, implying harmonic injection into the system. Such behaviour is typically observed in systems where the load is powered by **active converters, motor drives, or nonlinear electronic equipment**. This current distortion may necessitate the use of **harmonic filters or power quality improvement strategies** to prevent adverse effects on the power system, such as voltage distortion, overheating of equipment, or reduced system efficiency.

From a power system perspective, this case demonstrates the importance of maintaining voltage quality at the point of common coupling (PCC), even when the load exhibits nonlinear characteristics.

## Conclusion

The analytical investigation presented in this paper highlights the significance of coordinated power flow control for grid-connected PV-battery systems. Through detailed modelling and simulation, the study demonstrates how intelligent control of interfacing converters, in conjunction with energy storage, enhances operational efficiency and power quality in modern distribution networks.

Key findings emphasize that the combination of a fast and stable maximum power point tracking (MPPT) algorithm with a well-regulated battery interface ensures optimal utilization of solar energy while maintaining system stability. The PV subsystem, governed by MPPT, successfully tracks the maximum power point under rapidly changing irradiance, confirming the robustness of the controller against environmental variability. Concurrently, the battery exhibits effective voltage regulation and smooth current transitions, validating its role in balancing power fluctuations and supporting the grid during sudden load events. Shunt inverters play a critical role in sustaining voltage levels and mitigating harmonics at the point of common coupling. Their ability to inject or absorb reactive power, together with harmonic compensation, significantly improves voltage regulation and overall power quality. Grid-side voltage and current waveforms remain sinusoidal and well-synchronized, adhering to standard power quality indices even under nonlinear loading conditions. The results further reveal that load voltage quality is preserved despite the presence of distorted current profiles, a testament to the system's ability to isolate sensitive equipment from upstream disturbances. Voltage injection mechanisms, such as dynamic compensators, effectively counteract supply sags, ensuring continuous and reliable operation.

From a practical perspective, this study underlines the potential of integrated PV-battery systems to support grid resilience and facilitate higher renewable energy penetration without compromising supply quality. The control strategy proposed herein is scalable, making it suitable for residential micro grids, commercial installations, and utility-scale renewable plants. Future work may extend the analytical model by incorporating additional distributed resources, adaptive control schemes, and optimization algorithms for real-time energy management. Experimental validation on a hardware prototype will also be essential to confirm the feasibility of the proposed framework under real-world operating constraints. Overall, the research confirms that efficient power flow control in grid-connected PV-battery systems is pivotal for achieving a sustainable, reliable, and high-quality power supply. By integrating energy storage with advanced converter-based control, utilities and consumers can benefit from improved voltage stability, reduced harmonic content, and enhanced operational flexibility key attributes for the evolution of smart grids and renewable-based energy infrastructures.

## References

1. Naqvi, S. B. Q., & Singh, B. (2024). Weak grids are reintegrated with improved power quality pv-battery system with controlled power flow and grid assistive capabilities. *IEEE Transactions on Industry Applications*, 60(3), 4517-4529.
2. Mahir, O., Rochd, A., Benazzouz, A., & Ghennoui, H. (2024). Towards decarbonizing large-scale industries: A decision support framework for optimizing grid-connected PV-battery energy systems planning—Case study of an OCP mining site, Morocco, North Africa. *Heliyon*, 10(20).
3. Jain, A., & Bhullar, S. (2025). Design and performance analysis of solar PV-battery energy storage system integration with three-phase grid. *Journal of Power Sources*, 640, 236486.
4. Dankar, O., Tarnini, M., El Ghaly, A., Moubayed, N., & Chahine, K. (2025). A Neural Network-Based Model Predictive Control for a Grid-Connected Photovoltaic–Battery System with Vehicle-to-Grid and Grid-to-Vehicle Operations. *Electricity*, 6(2), 32.
5. Mouna, E. Q., Abbou, A., Laamim, M., Id-Khajine, L., & Rochd, A. (2025). Comparative Analysis of GA and PSO Algorithms for Optimal Cost Management in On-Grid Microgrid Energy Systems with PV-Battery Integration. *Global Energy Interconnection*.
6. Bishla, S., & Khosla, A. (2024). Honey badger optimized energy management in grid connected solar PV battery for enhancing the stability and power quality. *Energy Storage*, 6(1), e512.
7. Dinesh, M. N., & Eti, M. (2024, November). Optimized incremental conductance mppt for grid-connected pv systems with battery and supercapacitor integration. In *2024 8th International Conference on Computational System and Information Technology for Sustainable Solutions (CSITSS)* (pp. 1-6). IEEE.
8. Terkes, M., Demirci, A., Gokalp, E., & Cali, U. (2025). Impact analysis of battery control strategies on battery aging for grid-connected and solar-powered residential battery applications. *Heliyon*, 11(9).
9. Kar, M. K., Kanungo, S., Dash, S., & Parida, R. R. (2024). Grid connected solar panel with battery energy storage system. *Int. J. Appl.*, 13(1), 223-233.
10. Boruah, D., & Chandel, S. S. (2024). Techno-economic feasibility analysis of a commercial grid-connected photovoltaic plant with battery energy storage-achieving a net zero energy system. *Journal of Energy Storage*, 77, 109984.

11. Lachheb, A., Chrouta, J., Akoubi, N., & Salem, J. B. (2025). Enhancing efficiency and sustainability: a combined approach of ANN-based MPPT and fuzzy logic EMS for grid-connected PV systems. *Euro-Mediterranean Journal for Environmental Integration*, 1-13.
12. Agajie, T. F., Ibrahim, F. S., Amoussou, I., Agajie, E. F., Paddy, E. Y., Awoke, Y. A., ... & Bajaj, M. (2025). Comparative techno-economic analysis of grid-connected solar PV-battery and PV-fuel cell systems for educational institutions sustainable academic laboratories. *Discover Sustainability*, 6(1), 1-31.
13. Dufo-López, R., Lujano-Rojas, J. M., Artal-Sevil, J. S., & Bernal-Agustín, J. L. (2024). Optimising Grid-Connected PV-Battery Systems for Energy Arbitrage and Frequency Containment Reserve. *Batteries*, 10(12), 427.
14. Ishraque, M. F., Arafat, M. I., Ahmad, K., Shezan, S. A., Hossain, M. M., Amin, M. R., ... & Alenezi, A. H. (2025). Solar and battery-oriented grid connected microgrid for peak and off peak hour operation. *Results in Engineering*, 106766.
15. Panda, S., Rout, P. K., Sahu, B. K., Mbasso, W. F., Jangir, P., & Elrashidi, A. (2025). Optimization-Based Energy Management for Grid-Connected Photovoltaic–Battery Systems in Smart Grids Using Demand Response and Particle Swarm Optimization. *Engineering Reports*, 7(7), e70305.
16. Ahamd, W., & Ullah, I. (2025, February). Unified power quality conditioner based power quality improvement in microgrid. In *2025 IEEE Texas Power and Energy Conference (TPEC)* (pp. 1-6). IEEE.
17. Bashir, J., Ahmad, S., & Anees, A. S. (2024). Unified Power Quality Conditioner (UPQC) Based on Multilevel Configurations. *Multilevel Converters*, 233-251.
18. Farook, S., Vijayakumar, Y. N., Sridhar, S., Thrinath, B. S., Manohara, M., & Venkatesh, M. (2025, June). A Synchronized Unified Power Quality Conditioner For Hybrid Energy Storage Power Management. In *2025 International Conference on Computing Technologies (ICOCT)* (pp. 1-6). IEEE.
19. Jegatha, S. (2025, March). Improvement of power quality by a custom power device of unified power quality conditioner. In *AIP Conference Proceedings* (Vol. 3137, No. 1, p. 030006). AIP Publishing LLC.
20. Nishad, D. K., Tiwari, A. N., & Khalid, S. (2025). Multi-Objective Optimization Simulation of Unified Power Quality Conditioner (UPQC). *International Journal of Theoretical & Applied Computational Intelligence*, 71-83.
21. Rani, J., & Bhargava, A. (2024). Integrating Unified Power Quality Conditioners with Renewable Energy Sources: A Review of Performance Enhancements in Hybrid Systems. *Research Journal of Engineering Technology and Medical Sciences (ISSN: 2582-6212)*, 7(04).
22. Parmar, K., & Sarvaiya, J. Analysis & Function of Unified Power Quality Conditioner for Power Quality Improvement of Distributed Network.
23. Jagadeesh Kumar, M., Chandrasekar, P., Anand Bhat, B., & Gupta, S. (2025). Enhancing power quality in distribution networks using three-phase unified power quality conditioner (UPQC). *Environment, Development and Sustainability*, 1-23.
24. Qasim, A. Y., Tahir, F. R., & Alsammak, A. N. B. (2024). Improving Power Quality in Distribution Systems Using UPQC: An Overview. *Journal Européen des Systèmes Automatisés*, 57(2).
25. Rao, N. S., & Rao, P. V. R. A novel reduced-switch multi-level inverter based multi-device universal power-quality conditioner for PQ enhancement. *Int J Adv Appl Sci ISSN*, 2252(8814), 8814.
26. Shravani, C., & Narasimham, R. L. (2024). UPQC-Based power quality improvement in grid-linked PV, battery & wind systems. In *E3S Web of Conferences* (Vol. 547, p. 01007). EDP Sciences.
27. Prasada Rao, C. S., Pandian, A., Reddy, C. R., Bajaj, M., Massoud, J., & Shouran, M. (2024). Unified power quality conditioner-based solar EV charging station using the GBDT–JS technique. *Frontiers in Energy Research*, 12, 1343635.
28. Bharti, K., Singh, S. K., & Jha, S. K. (2023, May). Comparative study of ANN and incremental conductance MPPT for solar water pump. In *2023 International Conference on Recent Advances in Electrical, Electronics & Digital Healthcare Technologies (REEDCON)* (pp. 296-301). IEEE.
29. Bharti, K., Singh, S. K., Jha, S. K., & Gupta, R. (2023, January). Modelling and simulation of solar water pump using arduino uno in Proteus. In *2023 International Conference on Intelligent and Innovative Technologies in Computing, Electrical and Electronics (IITCEE)* (pp. 774-781). IEEE.
30. Kumar, B. A., Jyothi, B., Singh, A. R., & Bajaj, M. (2024). Enhancing EV charging predictions: a comprehensive analysis using K-nearest neighbours and ensemble stack generalization. *Multiscale and Multidisciplinary Modeling, Experiments and Design*, 7(4), 4011-4037.
31. Chandra, I., Singh, N. K., Samuel, P., Bajaj, M., & Zaitsev, I. (2024). Coordinated charging of EV fleets in community parking lots to maximize benefits using a three-stage energy management system. *Scientific Reports*, 14(1), 32026.
32. Srilakshmi, K., Rao, G. S., Balachandran, P. K., & Senju, T. (2024). Green energy-sourced AI-controlled multilevel UPQC parameter selection using football game optimization. *Frontiers in Energy Research*, 12, 1325865.
33. Srilakshmi, K., Rao, G. S., Swarnasri, K., Inkollu, S. R., Kondreddi, K., Balachandran, P. K., & Colak, I. (2024). Optimization of ANFIS controller for solar/battery sources fed UPQC using an hybrid algorithm. *Electrical Engineering*, 106(4), 3743-3770.
34. Borra, S. R., & Balachandran, P. K. (2024). Optimal design of solar/wind/battery and EV fed UPQC for. *Attainment of SDGs through the Advancement in Solar PV systems*, 24.

35. Srilakshmi, K., Gaddameedhi, S., Borra, S. R., Balachandran, P. K., Reddy, G. P., Palanivelu, A., & Selvarajan, S. (2024). Optimal design of solar/wind/battery and EV fed UPQC for power quality and power flow management using enhanced most valuable player algorithm. *Frontiers in Energy Research*, 11, 1342085.
36. Wu, T. H., Huang, S. S., & Chen, P. Y. (2024). Application of a three-phase unified power quality conditioner in a microgrid. *IET Smart Grid*, 7(6), 872-890.
37. Das, S. K., Swain, S. C., Dash, R., Reddy, J., Chinthaginjala, R., Jena, R., ... & ELrashidi, A. (2024). Design and analysis of UPQC in a microgrid using model reference adaptive control ensemble with back-stepping controller. *Heliyon*, 10(14).
38. Oliya, A. (2025). *Performance Evaluation Of PV-ESS-Integrated Grid Using ANN Tuned UPQC For Power Quality Enhancement* (Doctoral dissertation, IOE).